

Motion-Induced Radiation from a Dynamically Deforming Mirror

Faez Miri and Ramin Golestanian

Institute for Advanced Studies in Basic Sciences, Zanjan 45195-159, Iran

(October 5, 2018)

A path integral formulation is developed to study the spectrum of radiation from a perfectly reflecting (conducting) surface. It allows us to study arbitrary deformations in *space* and *time*. The spectrum is calculated to second order in the height function. For a harmonic traveling wave on the surface, we find many different regimes in which the radiation is restricted to certain directions. It is shown that high frequency photons are emitted in a beam with relatively low angular dispersion whose direction can be controlled by the mechanical deformations of the plate.

The Casimir effect [1] provides a direct link between the macroscopic world and the quantum vacuum. Imposing boundary conditions on the electromagnetic field in the space between two parallel conducting plates changes zero point vacuum fluctuations, and results in an attractive force between the plates. Dynamical modification of boundary conditions tends to perturb the quantum vacuum, leading to excitation of photons [2]. The corresponding *radiation reaction* results in a friction-like dissipative force. This is one of the manifestations of the so-called dynamic Casimir effect [3–6]. Dissipative forces also appear for nonideal conductors that move laterally [7]. However, they are fundamentally different, because in this case the dissipation mechanism is due to the Ohmic loss of the induced current in the bulk.

The emission of photons by a perfect cavity, and the observability of this energy, has been studied by different approaches [5,8]. The most promising candidate is the resonant production of photons when the mirrors vibrate at the optical resonance frequency of the cavity [9]. The radiation due to vacuum fluctuations of a collapsing dielectric sphere (bubble) has been studied and proposed as a possible explanation for the intriguing phenomenon of sonoluminescence [10]. Recently Maia Neto and Machado [11] studied the angular distribution and frequency spectrum of radiation from a single perfectly reflecting mirror with oscillatory motion. They found restrictions on the angular distribution of radiation, i.e. not all directions are allowed for the radiation.

The above calculations are for rigidly oscillating flat plates and spheres. In this paper, we have developed a path integral method to study the radiation from perfectly reflecting mirrors that undergo small dynamic deformations. We calculate the angular distribution and the total spectrum of radiation from a dynamically perturbed quantum vacuum. We examine the specific example of a single perfectly reflecting plate undulating harmonically with a frequency ω_0 and a wavevector \mathbf{k}_0 . We find that depending on the value of ω_0/k_0 , radiation at a frequency Ω can belong to different classes, each characterized by specific constraints on the angular distribution that restrict the radiation to a particular solid angle window. Radiation at frequencies close to ω_0 are restricted

to a single direction which is parallel to \mathbf{k}_0 and makes an angle $\theta_b = \sin^{-1}(k_0/\omega_0)$ with the surface normal. Hence, we can control the direction of emission as well as the frequency and the angular dispersion of the beam just by tuning (ω_0, \mathbf{k}_0) .

The total spectrum of radiation is found by integrating the angular distribution of radiation over the unit sphere. It is found to be a symmetric function with respect to $\omega_0/2$, where it is peaked. The peak sharpens as the parameter ω_0/k_0 is increased, and saturates for $k_0 = 0$. The connection between the dissipative dynamic Casimir force and radiation of photons is made explicit by calculating the total energy of photons radiated per unit time per unit area of the plate, which is identical to the energy dissipation rate calculated in Ref. [6]. We find that no radiation exists at frequencies higher than ω_0 , due to conservation of energy, and also for $\omega_0/k_0 < 1$ in agreement with Ref. [6] who find no dissipative forces for this regime.

The calculation is comprised of three steps. The LSZ formalism is used to relate the transition amplitude from an empty vacuum (at $t \rightarrow -\infty$) to a state with two photons (at $t \rightarrow +\infty$), to two-point correlation functions of the field. The two-point correlations can then be calculated perturbatively in the deformations using a path integral formulation. Finally, we obtain the radiation spectra by integrating over the state of one photon.

Our approach is a natural generalization of the path integral method developed by Golestanian and Kardar [6] to study mechanical response of vacuum. As in Ref. [6], we simplify the problem by considering a scalar field Φ (in place of the electromagnetic vector potential) with the action ($c = 1$)

$$S = \frac{1}{2} \int d^d X \partial_\mu \Phi(X) \partial_\mu \Phi(X), \quad (1)$$

where summation over $\mu = 1, \dots, d$ is implicit. Following a Wick rotation, imaginary time appears as another coordinate $X_d = it$ in the d -dimensional space-time. We would like to quantize the field subject to the constraints of its vanishing on a set of n manifolds (objects) defined by $X = X_\alpha(y_\alpha)$, where y_α parametrize the α th manifold.

Following Refs. [6,12], we can impose the constraints using delta functions, and calculate the two-point correlation function of the field as ($\hbar = 1$)

$$G(X, Y) = \int \mathcal{D}\Phi(X) \Phi(X)\Phi(Y) \quad (2)$$

$$\times \prod_{\alpha=1}^n \prod_{y_\alpha} \delta(\Phi(X_\alpha(y_\alpha))) e^{-S[\Phi]}.$$

Now consider a scattering process in which we start with a vacuum as the initial state, perturb it with dynamic boundary conditions during a finite period of time, and look for particles (that have possibly been created as a consequence of the perturbation) in the final state of the system. Using the LSZ reduction formalism [13], we can find the transition amplitude from the vacuum to a two photon state from the matrix elements of the S -matrix, as [14]

$$S_{fi} \equiv \langle k, k' | \hat{S} | 0 \rangle \quad (3)$$

$$= \frac{1}{2\sqrt{\Omega_k \Omega_{k'}}} \tilde{G}(k, \Omega_k; k', \Omega_{k'}) (k^2 - \Omega_k^2) (k'^2 - \Omega_{k'}^2),$$

where $k = (\mathbf{k}, k_z)$, and $\tilde{G}(k, \Omega; k', \Omega')$ is the Fourier transform of the two point function defined in Eq.(2), and $\Omega_k = \sqrt{\mathbf{k}^2 + k_z^2}$ denotes the photon dispersion relation in vacuum [15]. To obtain the distribution of radiation as measured by a detector, we need to sum over the momenta of the second photon. The angular distribution of radiated photons is given by $\mathcal{P}(\Omega, \theta, \phi) = (\Omega^2/8\pi^3) \int d^3k' / (2\pi)^3 |S_{fi}|^2$, and the total number of photons by $\mathcal{P}(\Omega) = \int d\cos\theta d\phi \mathcal{P}(\Omega, \theta, \phi)$, where θ and ϕ are the polar angles defining the direction of the emission of radiation.

The calculation of the two-point function in Eq.(2) is generally complicated since the Lagrange multiplier fields are defined on a set of manifolds with nontrivial geometry. To be specific, we focus on a 2d plate embedded in 3+1 space-time. Deformation of the plate is parametrized by the height function $h(\mathbf{x}, t)$ along the x_3 -axis, where $\mathbf{x} \equiv (x_1, x_2)$ denotes the two lateral space coordinates while t is the time variable. Generalizing the method of Ref. [6], we can calculate $G(X, Y)$ by a perturbative series in powers of the height function. The resulting expression for the Fourier transform of time ordered two point function reads

$$\tilde{G}(k, \Omega; k', \Omega') = \frac{2k_z \sqrt{\Omega'^2 - \mathbf{k}'^2} + 2k'_z \sqrt{\Omega^2 - \mathbf{k}^2}}{(\mathbf{k}^2 + k_z^2 - \Omega^2)(\mathbf{k}'^2 + k_z'^2 - \Omega'^2)} \quad (4)$$

$$\times \tilde{h}(\mathbf{k} + \mathbf{k}', \Omega + \Omega') + O(h^2),$$

to the leading order. The corresponding expression for the spectrum reads

$$\mathcal{P}(\Omega, \theta, \phi) = \int \frac{d\omega d^2\mathbf{q}}{(2\pi)^3} \mathcal{R}(\Omega, \theta, \phi; \mathbf{q}, \omega) |\tilde{h}(\mathbf{q}, \omega)|^2, \quad (5)$$

in which

$$\mathcal{R}(\Omega, \theta, \phi; \mathbf{q}, \omega) = \frac{\Omega}{2\pi^3} (\Omega^2 - \mathbf{k}^2) \sqrt{(\omega - \Omega)^2 - (\mathbf{q} - \mathbf{k})^2} \quad (6)$$

$$\times \Theta(\omega - \Omega) \Theta((\omega - \Omega)^2 - (\mathbf{q} - \mathbf{k})^2),$$

where $\mathbf{k} = (\Omega \sin\theta \cos\phi, \Omega \sin\theta \sin\phi)$, and $\Theta(x)$ is the Heaviside step function.

As a concrete example, let's consider a case where the deformation of the plate is in the form of a harmonic traveling wave. The height function can be represented as $h(\mathbf{x}, t) = d \cos(\mathbf{k}_0 \cdot \mathbf{x} - \omega_0 t)$ for a harmonic wave that propagates with the phase velocity ω_0/k_0 . This helps us study the optical response of vacuum to surface deformations in the frequency-wavevector domain. Most of the following analysis deals with the far from trivial problem of matching the spatial and temporal sinusoids characterizing the mirror to those characterizing the two plane-wave photons. This problem, which is essentially kinematic, has strong echoes of more familiar though somewhat simpler problems involving crystal and other gratings.

The angular distribution of radiated photons per unit time per unit area of the plate P , can be calculated from Eq.(6) as ($P \equiv \mathcal{P}/AT$)

$$P(\Omega, \theta, \phi) = \frac{d^2 \Omega}{4\pi^3} (\Omega^2 - \mathbf{k}^2) \sqrt{(\omega_0 - \Omega)^2 - (\mathbf{k}_0 - \mathbf{k})^2} \quad (7)$$

$$\times \Theta(\omega_0 - \Omega) \Theta((\omega_0 - \Omega)^2 - (\mathbf{k}_0 - \mathbf{k})^2).$$

The first step function in the above expression shows that the emitted photons can only have frequencies smaller than ω_0 . (The negative frequency Fourier component of the height function drops out due to similar constraints.) The second step function places some restrictions on the possible directions for emission of radiation, leading to a nontrivial angular distribution. If we take \mathbf{k}_0 to be parallel to the x_1 direction, the condition on possible directions for the radiation reads

$$(\omega_0 - \Omega)^2 > k_0^2 + \Omega^2 \sin^2\theta - 2k_0\Omega \sin\theta \cos\phi. \quad (8)$$

The above inequality can be most easily solved geometrically. Using the parametrization $(x, y, z) = (\sin\theta \cos\phi, \sin\theta \sin\phi, \cos\theta)$ for the unit director, the permissible directions for radiation can be represented as regions of the xyz -space that satisfy the following conditions: $[(\omega_0 - \Omega)/\Omega]^2 > (x - k_0/\Omega)^2 + y^2$, which corresponds to the interior of a cylinder with radius $r = (\omega_0 - \Omega)/\Omega$, and $x^2 + y^2 + z^2 = 1$ which corresponds to surface of a unit sphere. Hence, we simply need to find the intersection of the unit sphere and the cylinder. Depending on the radius of the cylinder and on the way they intersect many different cases may arise, each of which leading to a characteristic angular distribution of radiation. The partition of the parameter space into these different regions is summarized in Fig. 1.

In the special case $k_0 = 0$, there are two possibilities. For $r > 1$, the sphere is completely contained within

the cylinder, and there is no restriction for radiation. For $r < 1$, however, the intersection restricts the radiation zone to the circular patch defined by $\theta < \theta_0 = \sin^{-1}((\omega_0 - \Omega)/\Omega)$ [11]. In general k_0 is not zero, and there exist 7 interesting regimes: **(1)** For $k_0/\Omega < 1$, $r < 1 - k_0/\Omega$, and $r < k_0/\Omega$, the projection of the cylinder onto the xy -plane is completely contained within the unit circle, but it does not contain the origin. In this case all radiation is limited to $-\phi_{max} < \phi < \phi_{max}$, and (for a specific angle ϕ) $\theta_+(\phi) < \theta < \theta_-(\phi)$ where $\phi_{max} = \sin^{-1}[(\omega_0 - \Omega)k_0/\Omega^2] < \pi/2$, and

$$\theta_{\pm}(\phi) = \cos^{-1} \left\{ 1 - [(\omega_0 - \Omega)/\Omega]^2 - (k_0/\Omega)^2 \cos 2\phi \right. \\ \left. \pm 2(k_0/\Omega)^2 \cos \phi [(\omega_0 - \Omega)^2/k_0^2 - \sin^2 \phi]^{1/2} \right\}^{1/2}. \quad (9)$$

It is interesting to note that in this regime no radiation is emitted normal to the plate. In fact for $\Omega \sim \omega_0$ ($r \ll 1$), the radiation is limited to $\theta \approx \sin^{-1}(k_0/\omega_0)$, and $\phi \approx 0$. Furthermore, the beam will have a relatively low angular dispersion ($\sim r$). **(2)** In the regime $k_0/\Omega < 1$, and $1 - k_0/\Omega < r < k_0/\Omega$, the projection of the cylinder onto the xy -plane intersects with the unit circle with its center being inside, but it does not contain the origin. In this case there is a critical angle defined as

$$\phi_c = \cos^{-1} \left(\frac{1 - [(\omega_0 - \Omega)/\Omega]^2 + (k_0/\Omega)^2}{2k_0/\Omega} \right), \quad (10)$$

at which the behavior changes drastically. For $-\phi_c < \phi < \phi_c$, we have $\theta_+(\phi) < \theta < \pi/2$, while for $\phi_c < \phi < \phi_{max}$ or $-\phi_{max} < \phi < -\phi_c$, we have $\theta_+(\phi) < \theta < \theta_-(\phi)$. **(3)** When $r > 1 - k_0/\Omega$, and $k_0/\Omega < r < k_0/\Omega + 1$, the projection of the cylinder onto the xy -plane intersects with the unit circle, and contains the origin. In this case for $-\phi_c < \phi < \phi_c$, we have $0 < \theta < \pi/2$, and for $\phi_c < \phi < \pi$ or $-\pi < \phi < -\phi_c$, we have $0 < \theta < \theta_-(\phi)$. **(4)** In case $r > 1 + k_0/\Omega$, the projection of the cylinder onto the xy -plane completely contains the unit circle. Radiation can be detected in all directions with no restrictions, i.e. $0 < \theta < \pi/2$ and $0 < \phi < 2\pi$. **(5)** For $k_0/\Omega > 1$, and $r < k_0/\Omega - 1$, the projection of the cylinder onto the xy -plane is disjoint from the unit circle. No radiation exists in this case. **(6)** When $k_0/\Omega > 1$, and $k_0/\Omega - 1 < r < k_0/\Omega$, the projection of the cylinder onto the xy -plane intersects with the unit circle with its center being outside, but it does not contain the origin. Radiation is limited to $-\phi_c < \phi < \phi_c$ and $\theta_-(\phi) < \theta < \pi/2$. **(7)** Finally, for $k_0/\Omega < 1$, and $k_0/\Omega < r < 1 - k_0/\Omega$, the projection of the cylinder onto the xy -plane is completely contained within the unit circle, and it contains the origin. In this case we have $0 < \theta < \theta_-(\phi)$ for $0 < \phi < 2\pi$.

The dashed lines in Fig. 1 represent three different classes of trajectories that are characterized by the parameter ω_0/k_0 . In each class, radiation has peculiar angular distributions. The total number of photons radiated per unit time per unit area, $P(\Omega)$, is plotted for these

three different classes in Fig. 2. The curves are obtained by numerical integration of the angular distribution taking into account the complicated boundary conditions discussed above. The plots are symmetric with respect to $\Omega/\omega_0 = 1/2$, where they are peaked. The symmetry is a manifestation of the process being due to a two-photon emission. As ω_0/k_0 is increased, the peak becomes narrower and sharper until it saturates at $\omega_0/k_0 = \infty$ [16].

We can calculate the total radiated energy of photons per unit time per unit area to obtain the energy dissipation rate. Given the symmetry of the spectrum (the average frequency of the radiation is always $\omega_0/2$), we obtain $R = \int d\Omega \Omega P(\Omega) = (\omega_0/2) \int d\Omega P(\Omega)$. The energy dissipation rate can also be calculated from the mechanical reponse of the system [6], and it reads $R = (d^2\omega_0/720\pi^2)(\omega_0^2 - k_0^2)^{5/2}$. Conservation of energy requires the two methods to give the same result for the total number of radiated photons, namely it requires

$$\mathcal{N} = \int d\Omega \mathcal{P}(\Omega) = \frac{d^2cTA}{360\pi^2} (\omega_0^2/c^2 - k_0^2)^{5/2}, \quad (11)$$

where the factors of c are restored to allow estimation in physical units. The above identity was found to be true for each class, within the accuracy of our numerical integrations.

In conclusion, we have developed a path integral formulation to study the radiation from perfectly reflecting mirrors with dynamic fluctuations. Although its application to a simplest example lead to relatively rich and complicated behaviors, the method itself is quite general. Application of the method to various other geometries, such as a fluctuating wire in 3+1D space-time, two fluctuating plates, and arrays of such objects will be published elsewhere.

It is a pleasure to acknowledge M. Kardar, V. Karimipour, M.R.H. Khajepour, M. Khorrami, and A. Shariati for invaluable discussions and suggestions. We also wish to thank M. Kardar for a careful reading of the manuscript and giving critical comments. RG acknowledges support from NSF grant DMR-93-03667 during a visit to MIT.

-
- [1] H.B.G. Casimir, Proc. K. Ned. Akad. Wet. **51**, 793 (1948).
 - [2] G.T. Moore, J. Math. Phys. **11**, 2679 (1970).
 - [3] S.A. Fulling and P.C.W. Davies, Proc. R. Soc. London A **348**, 393 (1976); Proc. R. Soc. London A **356**, 237 (1977); L.H. Ford and A. Vilenkin, Phys. Rev. D **25**, 2569 (1982); P.A. Maia Neto and S. Reynaud, Phys. Rev. A **47**, 1639 (1993).
 - [4] M.-T. Jaekel and S. Reynaud, Phys. Lett. A **167**, 227 (1992); Quantum Opt. **4**,39 (1992).

- [5] G. Calucci, J. Phys. A: Math. Gen. **25**, 3873 (1992); C.K. Law, Phys. Rev. A **49**, 433 (1994); C.K. Law, Phys. Rev. Lett. **73**, 1931 (1994); V.V. Dodonov, Phys. Lett. A **207**, 126 (1995); G. Barton and C. Eberlein, Ann. Phys. (N.Y.) **227**, 222 (1993); O. Meplan and C. Gignoux, Phys. Rev. Lett. **76**, 408 (1996); A. Lambrecht, M.-T. Jaekel, and S. Reynaud, Phys. Rev. Lett. **77**, 615 (1996).
- [6] R. Golestanian and M. Kardar, Phys. Rev. Lett. **78**, 3421 (1997); Phys. Rev. A, in press (1998).
- [7] L.S. Levitov, Europhys. Lett. **8**, 499 (1989); V.E. Mkrтчian, Phys. Lett. A **207**, 299 (1995); G. Barton, Ann. Phys. (N.Y.) **245**, 361 (1996); J.B. Pendry, J. Phys. Condens. Matter **9**, 10301 (1997); C. Eberlein, Phys. World, **11**, 27 (1998); A. Dayo, W. Alnasrallah, and J. Krim, Phys. Rev. Lett. **80**, 1690 (1998).
- [8] D.F. Mundarain and P.A. Maia Neto, Phys. Rev. A **57**, 1379 (1998).
- [9] P. Davis, Nature **382**, 761 (1996).
- [10] C. Eberlein, Phys. Rev. Lett. **76**, 3842 (1996); Phys. Rev. A **53**, 2772 (1996); P. Knight, Nature **381**, 736 (1996).
- [11] P.A. Maia Neto and L.A.S. Machado, Phys. Rev. A **54**, 3420 (1996).
- [12] H. Li and M. Kardar, Phys. Rev. Lett. **67**, 3275 (1991); Phys. Rev. A **46**, 6490 (1992).
- [13] See for example: W. Greiner and J. Reinhardt, *Field Quantization* (Springer, Berlin, 1996).
- [14] It is important to note that there is no reason, *a priori*, why only two photon states should be created. Since the theory is free (Gaussian), Wick's theorem determines higher correlation functions as products of two point functions. Eq.(4) then implies that all the higher correlation functions, which describe transitions to higher photon states, vanish to the lowest order in perturbation theory in the deformation field. Had we considered higher order effects in the perturbation theory, it would have been necessary to include transition to multiple photon states, and the radiation spectrum would no longer have been symmetric with respect to $\omega_0/2$.
- [15] Note that the dispersion relation sets $(k^2 - \Omega_k^2)$ to zero, so we only get nonzero matrix elements in Eq.(3) if we have the same poles in the two point function.
- [16] In this case the analytical expression for the spectrum can be worked out as $P(\Omega) = (d^2\omega_0^4/128\pi^2)[1 - (2\Omega/\omega_0 - 1)^4 + (2\Omega/\omega_0 - 1)^2 \ln |2\Omega/\omega_0 - 1|]$. This expression is identical (within a factor of 2) to that obtained in Ref. [11] for the TE mode of the electromagnetic (EM) field for $\omega_0/k_0 = \infty$, and has no divergence at $\Omega/\omega_0 = 1/2$. Interestingly, the TM mode of the EM field is shown in Ref. [11] to have a logarithmic divergence at $\Omega/\omega_0 = 1/2$ for $\omega_0/k_0 = \infty$, which we anticipate to be rounded off for any finite ω_0/k_0 .

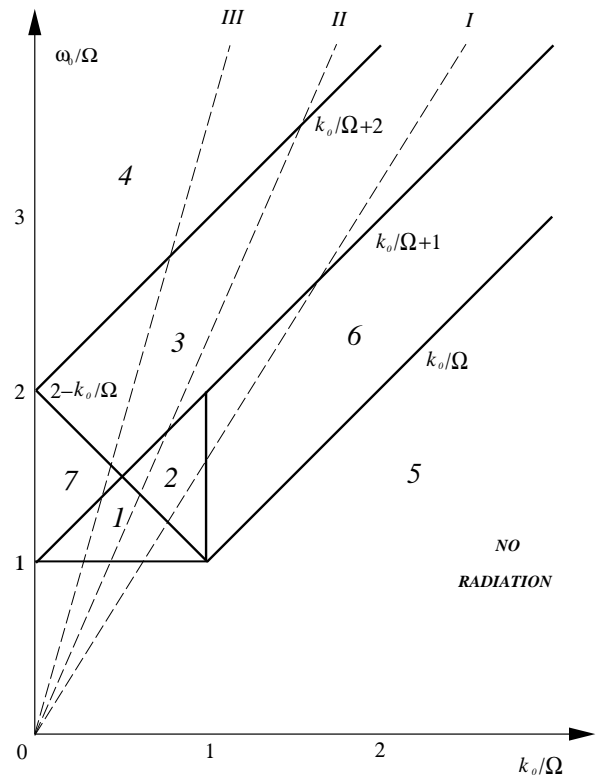


FIG. 1. Different regions in the frequency-wavevector plane. There is no radiation for $0 < \omega_0/k_0 < 1$. Class I corresponds to $1 < \omega_0/k_0 < 2$, class II corresponds to $2 < \omega_0/k_0 < 3$, and class III corresponds to $3 < \omega_0/k_0 < \infty$.

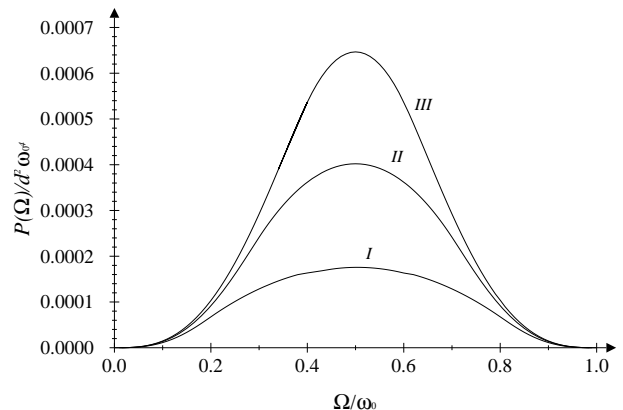


FIG. 2. Dimensionless spectrum of radiation $P(\Omega)/(d^2\omega_0^4)$ for different classes. Plot I corresponds to $\omega_0/k_0 = 5/3$, plot II corresponds to $\omega_0/k_0 = 5/2$, and plot III corresponds to $\omega_0/k_0 = 5$.